

Retraction and freezing of a water film on ice

Virgile Thiévenaz,^{1,2} Christophe Josserand,³ and Thomas Séon^{1,2}

¹*Sorbonne Universités, UPMC Université Paris 06, UMR 7190, Institut d'Alembert, F-75005 Paris, France*

²*CNRS, UMR 7190, Institut Jean Le Rond d'Alembert, F-75005 Paris, France*

³*Laboratoire d'Hydrodynamique (LadHyX), UMR 7646 CNRS-Ecole Polytechnique, IP Paris, F-91128 Palaiseau Cedex, France*



(Received 1 July 2019; revised manuscript received 22 December 2019;
accepted 20 March 2020; published 21 April 2020)

We investigate experimentally the different shapes taken by a water drop freezing during its impact on a cold surface. We show that these shapes are formed by a water film that remains on top of the first formed ice layer. The capillary hydrodynamics of this water film dewetting on its own ice, coupled with its vertical solidification, is thus quantitatively characterized, allowing us to understand and predict the formation of the emerging patterns. Finally, this experiment enables us to study the contact angle dynamics, giving deep insight into the wetting of water on ice.

DOI: [10.1103/PhysRevFluids.5.041601](https://doi.org/10.1103/PhysRevFluids.5.041601)

When a drop impacts a solid surface, it usually highly deforms, sometimes detaches droplets or bounces, and in all cases takes splendid shapes resulting from a subtle interplay between inertia, surface tension, viscosity, and substrate wetting. This iconic problem of fluid mechanics has been, and still is, extensively studied [1,2]. On the other hand, the freezing of a liquid sphere, considered in the mid-19th century as a model for the formation of Earth, probably constitutes the first solidification study of history [3,4], and keeps intriguing researchers today [5]. This Rapid Communication combines these two model problems to report on the unexpected shapes taken by frozen impacted drops, due to the interaction between the retraction of the drop after impact and its rapid freezing [6–8]. When solidification is coupled to the complex hydrodynamics of a drop impact [9], the geometry of the resulting frozen drop, called a splat in metallurgy, can be very diverse, showing in particular various shapes and roughnesses [10,11]. Knowing the shape of these splats is crucial as they enter in models of plasma spraying, a well-established means of forming thick coatings ($300\mu\text{m}$) useful in many applications (thermal protection, resistance to corrosion, oxidation, etc.) [7,12–14]. Even without impact, the simplest case of the freezing of a sessile drop on a cold surface already gives rise to a surprising pointy ice drop [15,16], raising the question of the contact angle between water and ice [17]. In order to understand these complex shapes, the behavior of a water film on ice has to be clarified, in particular, its retraction and wetting dynamics. Even though it has been the focus of a few studies [18,19], water capillary dynamics on ice still remains a highly complex subject, in particular because of the disordered quasiliquid layer on top of the surface of ice [20–23], which is affected by the surrounding gas composition [24], and explains ice slipperiness [25].

In this Rapid Communication, we investigate the retraction of liquid water on ice which occurs after a drop impacts a cold subfreezing surface. We show how the capillary hydrodynamics of a water film coupled with its solidification can build unexpected patterns (Fig. 1). Thus, we explore another way of studying the wetting of water on ice and of estimating the ice-water contact angle.

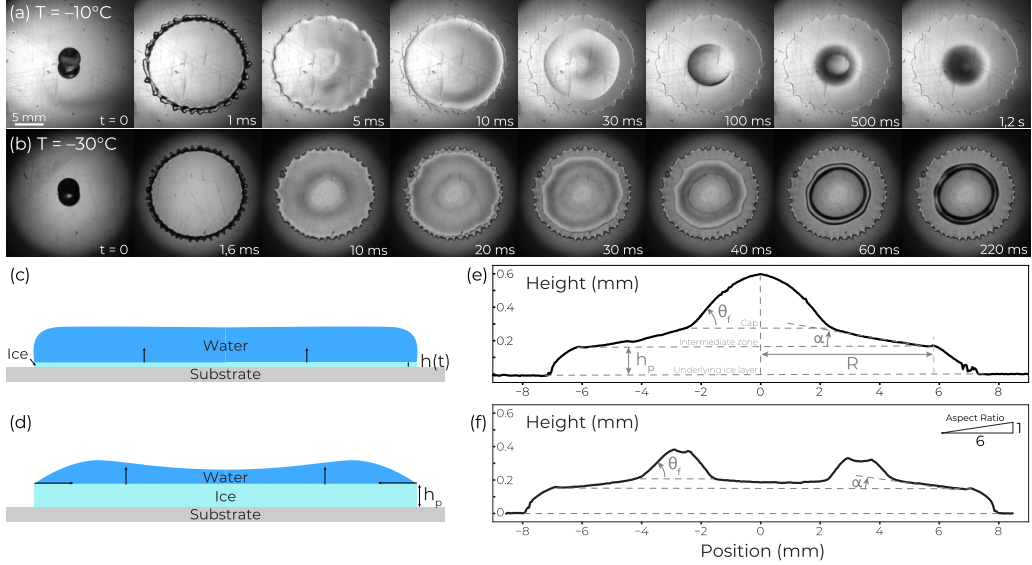


FIG. 1. (a) and (b) Image sequences of the impact and retraction of a water drop on a cold aluminum surface at two different temperatures. The liquid film starts retracting on ice about 10 ms after the impact. Depending on the substrate temperature [(a) -10°C ; (b) -30°C], the film will or will not have the time to fully retract, yielding different patterns (see the corresponding videos in SM [27]). (c) and (d) Schematic view of the first instants of a drop impacting a supercooled substrate, in particular, the ice and water dynamics. (e) and (f) Height profiles extracted from experiments similar to (a) and (b). The two ice structures will be referred as (a), (e) *cap* and (b), (f) *ring* patterns. All the geometrical quantities used in this Rapid Communication are defined here. The uncertainty Δh is of order $1\mu\text{m}$.

The drop impact setup consists of releasing a water drop at room temperature from a capillary tube using a syringe pump [26]. We consider two drop radii: $R_0 = 1.9$ and 1.2 mm . The impact velocity U_0 , controlled by the height of fall, ranges from 1.7 to 3 m s^{-1} . We use three large blocks ($100 \times 100 \times 30\text{ mm}$) of different materials (steel, copper, marble) as substrates, their distinct thermal properties [27] allowing us to change the rate of freezing [26,28,29]. They are cooled down between 0 and -80°C using liquid nitrogen. This experiment is placed inside a dry air chamber in order to minimize the frost formation. The impact dynamic is studied using a high-speed camera, and the height profile of the frozen drop is extracted with a polychromatic confocal sensor moving along a translation platform [27].

The impact process is represented by two timelines [Figs. 1(a) and 1(b)] corresponding to two different substrate temperatures, -10 and -30°C [see the corresponding videos in the Supplemental Material (SM) [27]]. In the first milliseconds of the impact the drop spreads and reaches its maximal diameter while a thin layer of ice freezes beneath it. Before the third image of each sequence, the system is in the configuration described by Fig. 1(c): The liquid film is pinned at the edge of a thin ice layer. Freezing goes on and the ice layer thickness follows the classical self-similar law $h(t) = \sqrt{D_{\text{eff}}t}$ given by solving the Stefan problem [4]. This latter considers a solidification front propagating between two phases (liquid and solid) of the same material, without a substrate. D_{eff} is the effective diffusion coefficient of the propagation dynamics of the ice-water front solidification. As shown in a previous article [26] and used here, an excellent estimation of the effective diffusion coefficient D_{eff} may be obtained by taking into account the heat propagation in the substrate. In the fourth image, the contact angle has relaxed down to its dewetting value [Fig. 1(d)] and the thickness of the ice layer at this point is called h_p .

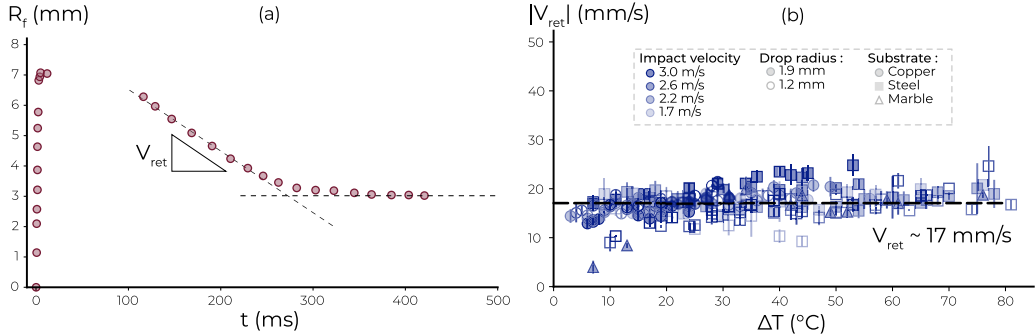


FIG. 2. (a) Time evolution of the liquid film radius R_f for a single experiment. R_f decreases linearly during the retraction, therefore pointing at a constant retraction velocity V_{ret} . (b) Retraction velocity of the water film on ice, as a function of $\Delta T = T_m - T_s$, for a large set of experiments with a Weber number ranging from 48 to 234. The top inset shows the meaning of the different markers: Impact velocities are represented by different colors (from dark blue for the fastest to light blue for the slowest), substrates by symbols (circles for copper, squares for steel, and triangles for marble), and drop radii by the filling (solid symbols for $R_0 = 1.9$ mm, open symbols for $R_0 = 1.2$ mm). The retraction velocity does not vary with the control parameters nor with the film thickness.

Between the fourth and sixth images the liquid retracts on ice, leading to two different shapes: a spherical cap [Fig. 1(a)] or a half ring [Fig. 1(b)] of water on top of a thin ice disk. Finally, the remaining liquid finishes freezing quasistatically, over a few hundreds of milliseconds. The retraction of a liquid on its own solid phase is not *a priori* expected thermodynamically; this is in fact not observed for molten metal or wax drop impacts [30,31] and seems to be a peculiar feature of water. It indicates in particular that liquid water and ice exhibit a nonzero contact angle as it has already been observed in a few other configurations [17,32–34].

As a consequence of this competition between capillary retraction and solidification, the different shapes adopted by the frozen drop depend on the impact parameters and the substrate temperature. For a constant set of impact parameters, when the substrate temperature is slightly below the melting temperature, the frozen structure takes the shape of a spherical cap on top of a thin disk, whereas when the substrate temperature is colder, the final shape is a half ring. Figures 1(e) and 1(f) present the height profiles corresponding to the two shapes and define the notations used in the following. Note that the aspect ratio of these two figures is 6, meaning that these ice structures are really flat: typically a few hundreds of microns thick and about 1 cm wide. On both profiles we can observe three different zones: the underlying ice layer of thickness h_p , the pattern on the top, which can be a spherical cap [Fig. 1(e)] or a ring [Fig. 1(f)], and an intermediate zone. We define the angle α as the angle between the ice-air interface and the horizontal in the intermediate zone, and the angle θ_f between the pattern and the horizontal. In the following, our goal is to quantitatively characterize the formation of such ice structures from the generic configuration of Fig. 1(d) and, in particular, to discuss the final angle θ_f on the solid structure.

Let us first consider the retraction of the water film on the ice disk. Figure 2(a) presents the film radius versus time showing that the retraction velocity V_{ret} is constant during most of the retraction. Subsequently, the retraction velocity is plotted in Fig. 2(b) for each experiment versus $\Delta T = T_m - T_s$, with T_m the melting temperature— 0°C in our case—and T_s the substrate temperature. We observe that V_{ret} is roughly the same for any value of the control parameters, represented by different markers: It does not vary with impact velocity, drop radius, substrate material, and temperature. Hence, we deduce the retraction velocity of water on ice,

$$V_{\text{ret}} \simeq 17 \pm 3 \text{ mm s}^{-1}. \quad (1)$$

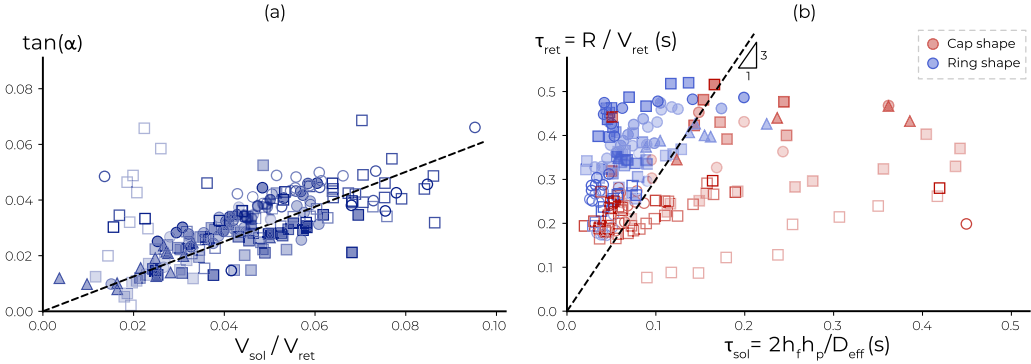


FIG. 3. Interactions between retraction and solidification. (a) Tangent of angle α as defined in Figs. 1(e) and 1(f), vs of the ratio of the solidification and the retraction velocities $V_{\text{sol}}/V_{\text{ret}}$. The set of experiments is the same as in Fig. 2(b) and the legend is also identical. The dashed line is the best linear fit with a slope 0.67. (b) Phase diagram of the possible final shapes, *cap* [red, see Fig. 1(a)] and *ring* [blue, see Fig. 1(b)], depending on the characteristic times of solidification τ_{sol} and retraction τ_{ret} . The symbol shapes and opacities represent the impact and freezing parameters, according to the legend in Fig. 2(b). The dashed line has a slope of 3 and is to guide the eye.

Yet, those control parameters do have an effect on the thickness of the liquid film which retracts on ice, which means that V_{ret} does not depend on the film thickness. As the film thickness appears in the Taylor-Culick velocity [35] [$\sqrt{\gamma/(\rho h_f)}$], this observation suggests that the capillary retraction is here balanced by viscosity, rather than by inertia.

In our experiment the ice keeps growing as long as there is water on it, so that the liquid film freezes as it retracts. The interplay between capillary retraction and solidification therefore controls the final shape of the frozen drop, and may be characterized by comparing the dynamics of both processes, which we do through scaling laws. Knowing the growth dynamics of ice [$h(t) = \sqrt{D_{\text{eff}}t}$], we can determine the solidification velocity V_{sol} [$dh/dt = \sqrt{D_{\text{eff}}}/(2\sqrt{t})$] at the moment water starts retracting ($t = h_p^2/D_{\text{eff}}$),

$$V_{\text{sol}} = \frac{D_{\text{eff}}}{2h_p}. \quad (2)$$

Figure 3(a) shows the variation of $\tan(\alpha)$ [see Figs. 1(e) and 1(f)] versus the ratio of the solidification and retraction velocities, for all our experiments. All the data gather along a line $\tan \alpha \simeq 0.67V_{\text{sol}}/V_{\text{ret}}$, which demonstrates that the ice slope α is indeed the result of the balance between vertical solidification and radial retraction. The less-than-one 0.67 factor is probably due to an overestimation of V_{sol} , as it is defined at the beginning of the retraction whereas the real instant velocity decreases over time.

Now, we question the mechanism that selects the final pattern: cap [Fig. 1(e)] or ring [Fig. 1(f)]. We observe on the timelines [Figs. 1(a) and 1(b)] that during the relaxation of the contact line [between the second and fourth image, schematized by the transition from Fig. 1(c) to 1(d)], a rim appears at the edge of the liquid film creating a trough at the center [36,37]. When this film with a curved free surface retracts, two options exist: Either the freezing rate is slow compared to the retraction and the rim will eventually collapse into a cap shape [Figs. 1(a) and 1(e)], or either the freezing is quick enough to reach the trough before the rim collapses, in which case a liquid ring is left to freeze, yielding the ring shape [Figs. 1(b) and 1(f)]. In order to study the transition from one shape to another, the timescales of retraction τ_{ret} and solidification τ_{sol} can be estimated using the characteristic lengths R and h_f , respectively, the liquid film radius and thickness at the onset of

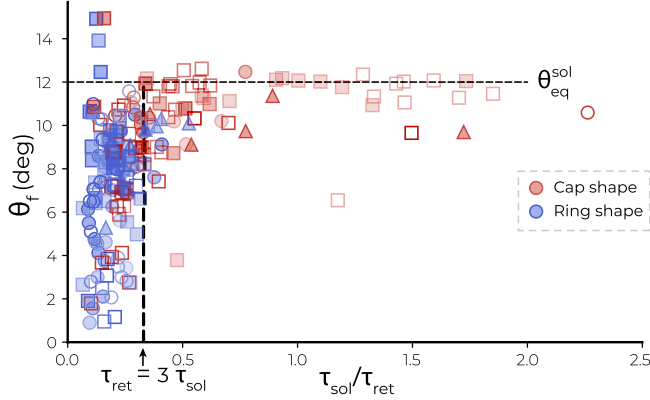


FIG. 4. Final contact angle θ_f of the retracting water film on ice vs the ratio of the characteristic times of solidification and retraction: $\tau_{\text{sol}}/\tau_{\text{ret}}$. For low values of this time ratio, θ_f varies between 1° and 12° . For high values of this time ratio, θ_f reaches a constant value $\theta_f = 12^\circ \pm 1^\circ$. The vertical dashed line shows a threshold that delimited the two ice shapes: $\tau_{\text{ret}}/\tau_{\text{sol}} = 3$, as in Fig. 3(b). The symbol shapes and opacities represent the impact and freezing parameters, according to the legend in Fig. 2(b).

retraction, measured from the thickness profiles (see more details in SM [27]), yielding

$$\tau_{\text{ret}} = \frac{R}{V_{\text{ret}}} \quad \text{and} \quad \tau_{\text{sol}} = \frac{h_f}{V_{\text{sol}}} = \frac{2h_f h_p}{D_{\text{eff}}}. \quad (3)$$

Figure 3(b) is a phase diagram that plots the timescales τ_{ret} vs τ_{sol} for our large range of control parameter values [see the legend in Fig. 2(b)], by distinguishing the cap (in red) and ring (in blue) experiments. We obtain a clear separation between the two shapes, shown with a dashed line, validating the proposed mechanism of pattern selection. The dashed line has a slope of 3, larger than 1, which may be explained through two distinct contributions: the use of the film radius R that overestimates τ_{ret} since the film only retracts on a fraction of it, and the previously described overestimation of V_{sol} which translates into an underestimation of τ_{sol} .

The main exception to our criterion concerns the group of open red markers in the lower left-hand side of Fig. 3(b), which represents a series of impacts with small drops yielding a cap shape (red) whereas they should yield a ring shape (blue). This mismatch can be understood as the effect of the small width of the retracting liquid film which results from the impact of smaller drops: If the film is not spread enough no rim will form, and therefore no ice ring will freeze, regardless of the solidification time. However, although this explanation qualitatively explains our data, we have unfortunately not been able to find a simple criterion quantifying the minimal size required to form a retraction rim.

Either way, the scaling analyses presented in Fig. 3 prove that the final shape of the frozen drop, be it the angle α or the pattern, ring or cap, is entirely defined by the competition between retraction and solidification. Note that another shape with two concentric rings instead of one can be observed, but this configuration is the result of the same mechanism that forms one ring.

Finally, this experiment provides an original way to progress on the wetting of water on ice. Indeed, the angle θ_f [Figs. 1(e) and 1(f)] is related to the contact angle that water made with ice at the moment it has been frozen, even if it probably only gives an indirect measurement of the real contact angle. Indeed, the density variation during solidification might change this angle. Moreover, we may wonder whether the solid-liquid interface is horizontal during the solidification, although it seems supported by the simple relation between $\tan \alpha$, V_{ret} , and V_{sol} [Fig. 3(a)].

Figure 4 presents the variation of θ_f for all our experiments, versus the ratio of the characteristic times of solidification τ_{sol} and retraction τ_{ret} . We first observe a whole range of θ_f from less than

1° up to about 15° in the ring configuration ($\tau_{\text{ret}} > 3\tau_{\text{sol}}$), when the film is solidified while it is retracting. Note that, as the retraction velocity is constant (Fig. 2), we would expect a constant value of the corresponding retraction angle that we do not observe on this graph. Indeed, in this case the receding contact line is frozen by the solidification front before water reached an equilibrium shape. Consequently, one should expect a strong modification of the water-ice angle due to the capillary relaxation of the remaining liquid being faster than the solidification front propagation. This relaxation dynamics while freezing explains the difference between θ_f and the real contact angle, and this difference should depend on the experimental parameters and is difficult to predict. However, when the water film has time to form an equilibrium spherical cap before being frozen ($\tau_{\text{ret}} < 3\tau_{\text{sol}}$), its contact angle with the ice always reaches a constant limit value, for any control parameters. Depending on whether or not a contact angle hysteresis exists [38], this particular angle may be an equilibrium angle or a retraction angle, but in either case it exists, is unique, and constant. Its value when solidified is called the solidified equilibrium angle $\theta_{\text{eq}}^{\text{sol}}$.

Despite the difference between the real contact angle and θ_f , it is interesting to compare our value $\theta_{\text{eq}}^{\text{sol}} \sim 12^\circ$ with those reported previously in the literature. In fact, to our knowledge, only a few studies have studied the ice-water contact angle and their results span a large range from 1° up to 40° [18,19,32–34,39,40]. In 1966, Knight [32] notably measured 12° for the receding contact angle of water on ice by observing the retraction of a freezing puddle. On the other hand, as the interfacial tension between ice and water is very low due to their high affinity [34], Young's relation imposes that a nonzero contact angle of water on ice is equivalent to a surface free energy of ice lower than the surface tension of water at 0°C , 75.6 mJ/m^2 [41]. Van Oss *et al.* [34] found accordingly that the surface free energy of ice is 69.2 mJ/m^2 , which puts the contact angle of water on ice around 24° . Our value of $\theta_{\text{eq}}^{\text{sol}}$ is therefore consistent with this range of value, but still does not help to discriminate between the preceding observations. However, if the relation between our solid equilibrium contact angle $\theta_{\text{eq}}^{\text{sol}}$ and the real ice-water contact angle can be estimated by further research, this experiment would provide another value of the contact angle of water on ice.

As a conclusion, the final shape of the frozen drop is determined by the competition between the dynamics of retraction and freezing. Moreover, our experiments enable us to characterize the retraction of water on ice, in terms of retraction velocity and wetting. We showed in particular that the water film retracts at a constant velocity which does not depend on the temperature nor on the film thickness. This study also outlines the contact angle dynamics during the retraction of water on ice and provides an alternative setup to characterize the equilibrium contact angle in the future. Further investigations into this wetting dynamic, especially its possible link to the surface melting of ice [33], might shed more light on the nature of the surface of ice [42].

-
- [1] A. M. Worthington, On the forms assumed by drops of liquids falling vertically on a horizontal plate, *Proc. R. Soc. London* **25**, 261 (1877).
 - [2] C. Josserand and S. T. Thoroddsen, Drop impact on a solid surface, *Annu. Rev. Fluid Mech.* **48**, 365 (2016).
 - [3] G. Lamé and B. P. Clapeyron, Mémoire sur la solidification par refroidissement d'un globe liquide, *Ann. Chim. Phys.* **47**, 250 (1831).
 - [4] L. I. Rubinstein, *The Stefan Problem*, Translations of Mathematical Monographs Vol. 27 (American Mathematical Society, Providence, RI, 1971).
 - [5] S. Wildeman, S. Sterl, C. Sun, and D. Lohse, Fast Dynamics of Water Droplets Freezing from the Outside In, *Phys. Rev. Lett.* **118**, 084101 (2017).
 - [6] S. D. Aziz and S. Chandra, Impact, recoil and splashing of molten metal droplets, *Int. J. Heat Mass Transfer* **43**, 2841 (2000).
 - [7] R. Dhiman, A. G. McDonald, and S. Chandra, Predicting splat morphology in a thermal spray process, *Surf. Coat. Technol.* **201**, 7789 (2007).

- [8] E. Ghabache, C. Josserand, and T. Séon, Frozen Impacted Drop: From Fragmentation to Hierarchical Crack Patterns, *Phys. Rev. Lett.* **117**, 074501 (2016).
- [9] I. V. Roisman, Fast forced liquid film spreading on a substrate: Flow, heat transfer and phase transition, *J. Fluid Mech.* **656**, 189 (2010).
- [10] R. Dhiman and S. Chandra, Freezing-induced splashing during impact of molten metal droplets with high Weber numbers, *Int. J. Heat Mass Transfer* **48**, 5625 (2005).
- [11] S. Chandra and P. Fauchais, Formation of solid splats during thermal spray deposition, *J. Thermal Spray Technol.* **18**, 148 (2009).
- [12] J. Madejski, Solidification of droplets on a cold surface, *Int. J. Heat Mass Transfer* **19**, 1009 (1976).
- [13] R. Bhola and S. Chandra, Parameters controlling solidification of molten wax droplets falling on a solid surface, *J. Mater. Sci.* **34**, 4883 (1999).
- [14] P. Fauchais, A. Vardelle, M. Vardelle, and M. Fukumoto, Knowledge concerning splat formation: An invited review, *J. Thermal Spray Technol.* **13**, 337 (2004).
- [15] W. W. Schultz, M. G. Worster, and D. M. Anderson, Solidifying sessile water droplets, in *Interactive Dynamics of Convection and Solidification*, edited by S. H. Davis, H. E. Huppert, U. Müller, and M. G. Worster, NATO Advanced Studies Institute, Series E: Applied Sciences (Springer, Berlin, 2001), Vol. 219, pp. 209–226.
- [16] A. G. Marin, O. R. Enriquez, P. Brunet, P. Colinet, and J. H. Snoeijer, Universality of Tip Singularity Formation in Freezing Water Drops, *Phys. Rev. Lett.* **113**, 054301 (2014).
- [17] D. M. Anderson, M. G. Worster, and S. H. Davis, The case for a dynamic contact angle in containerless solidification, *J. Cryst. Growth* **163**, 329 (1996).
- [18] C. A. Knight, Experiments on the contact angle of water on ice, *Philos. Mag.* **23**, 153 (1971).
- [19] V. F. Petrenko and R. W. Whitworth, *Physics of Ice* (Clarendon Press, Oxford, U.K., 1999).
- [20] J. W. M. Frenken and J. F. Van der Veen, Observation of Surface Melting, *Phys. Rev. Lett.* **54**, 134 (1985).
- [21] A. Lied, H. Dosch, and J. H. Bilgram, Surface Melting of Ice I_h Single Crystals Revealed by Glancing Angle X-Ray Scattering, *Phys. Rev. Lett.* **72**, 3554 (1994).
- [22] Y. Li and G. A. Somorjai, Surface premelting of ice, *J. Phys. Chem. C* **111**, 9631 (2007).
- [23] G. Sazaki, S. Zepeda, S. Nakatsubo, M. Yokomine, and Y. Furukawa, Quasi-liquid layers on ice crystal surfaces are made up of two different phases, *Proc. Natl. Acad. Sci. U.S.A.* **109**, 1052 (2012).
- [24] M. Elbaum, S. G. Lipson, and J. G. Dash, Optical study of surface melting on ice, *J. Cryst. Growth* **129**, 491 (1993).
- [25] R. Rosenberg, Why is ice slippery? *Phys. Today* **58**(12), 50 (2005).
- [26] V. Thiévenaz, T. Séon, and C. Josserand, Solidification dynamics of an impacted drop, *J. Fluid Mech.* **874**, 756 (2019).
- [27] See Supplemental Material at <http://link.aps.org/supplemental/10.1103/PhysRevFluids.5.041601> for details on the experimental setup and material properties, as well as videos of the two-impact regime.
- [28] T. Bennett and D. Poulikakos, Heat transfer aspects of splat-quench solidification: Modelling and experiment, *J. Mater. Sci.* **29**, 2025 (1994).
- [29] J. de Ruiter, D. Soto, and K. K. Varanasi, Self-peeling of impacting droplets, *Nat. Phys.* **14**, 35 (2018).
- [30] S. Schiaffino and A. A. Sonin, Motion and arrest of a molten contact line on a cold surface: An experimental study, *Phys. Fluids* **9**, 2217 (1997).
- [31] S. Schiaffino and A. A. Sonin, Molten droplet deposition and solidification at low Weber numbers, *Phys. Fluids* **9**, 3172 (1997).
- [32] C. A. Knight, The contact angle of water on ice, *J. Colloid Interface Sci.* **25**, 280 (1966).
- [33] L. Makkonen, Surface melting of ice, *J. Phys. Chem. B* **101**, 6196 (1997).
- [34] C. J. Van Oss, R. F. Giese, R. Wentzek, J. Norris, and E. M. Chuvalin, Surface tension parameters of ice obtained from contact angle data and from positive and negative particle adhesion to advancing freezing fronts, *J. Adhes. Sci. Technol.* **6**, 503 (1992).
- [35] F. E. C. Culick, Comments on a ruptured soap film, *J. Appl. Phys.* **31**, 1128 (1960).
- [36] M. Rivetti, T. Salez, M. Benzaquen, E. Raphaël, and O. Bäumchen, Universal contact-line dynamics at the nanoscale, *Soft Matter* **11**, 9247 (2015).

- [37] A. M. J. Edwards, R. Ledesma-Aguilar, M. I. Newton, C. V. Brown, and G. McHale, Not spreading in reverse: The dewetting of a liquid film into a single drop, *Sci. Adv.* **2**, e1600183 (2016).
- [38] D. Bonn, J. Eggers, J. Indekeu, J. Meunier, and E. Rolley, Wetting and spreading, *Rev. Mod. Phys.* **81**, 739 (2009).
- [39] W. M. Ketcham and P. V. Hobbs, An experimental determination of the surface energies of ice, *Philos. Mag.* **19**, 1161 (1969).
- [40] J. Drelich, E. Chibowski, D. D. Meng, and K. Terpilowski, Hydrophilic and superhydrophilic surfaces and materials, *Soft Matter* **7**, 9804 (2011).
- [41] D. R. Lide, *CRC Handbook of Chemistry and Physics* (CRC Press, Boca Raton, FL, 2005).
- [42] Y. Nagata, T. Hama, E. H. G. Backus, M. Mezger, D. Bonn, M. Bonn, and G. Sazaki, The surface of ice under equilibrium and nonequilibrium conditions, *Acc. Chem. Res.* **52**, 1006 (2019).